Journal of Applied Mechanics and Technical Physics, Vol. 37, No. 6, 1996

ON DETERMINING THE MECHANICAL PROPERTIES OF NONLINEAR-ELASTIC COMPOSITE MATERIALS

I. G. Teregulov, Yu. I. Butenko, R. A. Kayumov, D. Kh. Safiullin, and K. P. Alekseev

UDC 539.3

Experimental determination of mechanical properties of unidirectionally reinforced composite materials (UCM) involves well-known difficulties due to the fact that materials in the form of tapes and braids have small transverse dimensions. Moreover, the behavior of UCM as structural members differs from that in independent tests.

In this paper, we consider an approach that allows one to obtain information on the mechanical properties of a composite from experimental tests of structures made of this composite material (CM) [1–3]. The plane stress state of CM entering into a multilayer structure is studied. Examples of such structures are thin shells formed by winding or application of CM. However, certain difficulties arise here. They are due to the fact that, when the elastic moduli are greatly different, the desired small quantities (for example, ν_{12}, E_2, and G) change significantly with small variations of initial experimental data [3]. Problems of processing experimental data for nonlinear elasticity are studied, the calculation results of test problems are analyzed, and conditions imposed on an experiment are formulated.

1. We formulate the necessary relations obtained in [2]. We investigate objects such as thin multilayer plates and shells formed by application or winding of reinforced orthotropic layers. We relate the Cartesian coordinate system x^1, x^2 to a reinforced layer by directing the x^1 axis along the axis of orthotropy having maximum stiffness and the x^2 axis perpendicular to the x^1 axis in the plane of the layer (Fig. 1).

The relationship between stresses $\tilde{\sigma}^{\alpha\beta}$ and strains $\tilde{e}_{\alpha\beta}$ in an arbitrary coordinate system $\tilde{x}^1$, $\tilde{x}^2$ obtained from the system x^1x^2 by rotation about the x^3 axis in the plane of the tape for small strains is expressed in tensor form as

$$\tilde{\sigma}^{\alpha\beta} = A_1(\tilde{g}^{\alpha\beta} + \tilde{\Lambda}^{\alpha\beta}) + A_3(\tilde{g}^{\alpha\beta} - \tilde{\Lambda}^{\alpha\beta}) + 2A_2(\tilde{e}^{\alpha\beta} - (1/2)\tilde{g}^{\alpha\beta}\tilde{e}^{\rho}_{\rho} - (1/2)\tilde{\Lambda}^{\alpha\beta}\tilde{\Lambda}^{\rho\gamma}\tilde{e}_{\rho\gamma}) \quad (\alpha, \beta = 1, 2). \tag{1.1}$$

Here $\tilde{g}^{\alpha\beta}$ are the components of the metric tensor in the plane of a single tape; $\tilde{\Lambda}^{\alpha\beta}$ is a special tensor which has components $\Lambda^{11} = 1$, $\Lambda^{22} = -1$, and $\Lambda^{12} = \Lambda^{21} = 0$ in the coordinate system x^1, x^2; $\tilde{\sigma}^{\alpha\beta}$ and $\tilde{e}_{\alpha\beta}$ are the components of the stress and strain tensors of the tape in the system $\tilde{x}^1$, $\tilde{x}^2$; $A_i = A_i(I_1, I_2, I_3)$ are functions that characterize the elastic properties of the composite material, where $i = 1$, 2, and 3; and I_k are invariants of the form

$$I_1 = \tilde{e}^{\cdot\alpha}_{\alpha} + \tilde{\Lambda}^{\alpha\beta}\tilde{e}_{\alpha\beta}, \quad I_3 = \tilde{e}^{\cdot\alpha}_{\alpha} - \tilde{\Lambda}^{\alpha\beta}\tilde{e}_{\alpha\beta}, \quad I_2 = \tilde{e}_{\alpha\beta}\tilde{e}^{\alpha\beta} - (1/2)(\tilde{e}^{\cdot\alpha}_{\alpha})^2 - (1/2)(\tilde{\Lambda}^{\alpha\beta}\tilde{e}_{\alpha\beta})^2. \tag{1.2}$$

In the system x^1x^2 the stresses (1.1) and invariants (1.2) assume the form

$$\sigma^{11} = 2A_1, \quad \sigma^{22} = 2A_3, \quad \sigma^{12} = 2A_2e_{12}; \tag{1.3}$$

$$I_1 = 2e_{11}, \quad I_3 = 2e_{22}, \quad I_2 = 2e_{12}^2. \tag{1.4}$$

Below, we study materials whose longitudinal, transverse, and shearing stiffnesses differ greatly.

An asymptotic analysis of constitutive relations (1.1) for materials of this class was performed by Teregulov [2]. This made it possible to reduce the number of arguments of functions that characterize the

Kazan' State Architect-Building Academy, Kazan' 420043. Translated from Prikladnaya Mekhanika i Tekhnicheskaya Fizika, Vol. 37, No. 6, pp. 170–180, November–December, 1996. Original article submitted July 21, 1995.

0021-8944/96/3706-0917 $15.00

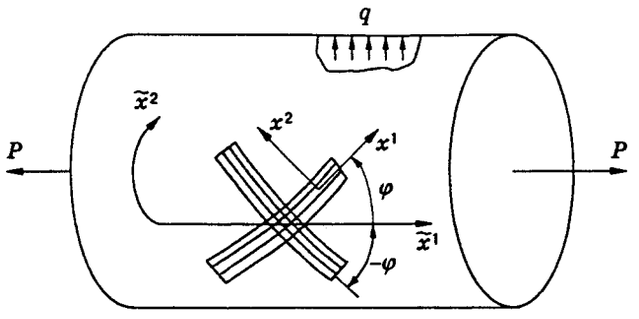

Fig. 1

stiffness of the nonlinear-elastic CM and to express these functions, with error $O(\eta^2)$ compared with unity, in the form

$$A_1(I_1, I_3) = A_{11}(I_1)I_1 + A_{13}(I_1)I_3, \quad A_3(I_1, I_3) = A_{31}(I_1)I_1 + A_{33}(I_3)I_3, \quad A_2(I_2) = A_2(I_2). \tag{1.5}$$

Moreover, the elastic characteristics A_{13} and A_{31} are related by

$$\frac{\partial A_{31}}{\partial I_1} I_1 + A_{31} = A_{13}. \tag{1.6}$$

2. Determination of A_i is based on processing of the results of experiments on tubular specimens (shells) formed by winding of a reinforced material at angles $\pm\varphi$ with respect to the generatrix. This allows one to take into account the specific behavior of CM constituents in the composition and also to take into account indirectly the influence of technological factors on the CM properties (a similar approach was used, for example, in [4, 5] to determine the mechanical properties of a linear-elastic CM). Loading is performed by an internal pressure and an axial force. We assume that the number of layers is sufficiently large and, hence, the strain of the shell is axisymmetric [4].

As the $\tilde{x}^1$ and $\tilde{x}^2$ axes, we choose the lines coinciding in direction with the meridian $\tilde{x}^1$ and the parallel $\tilde{x}^2$ of the shell of revolution.

The tensors $\tilde{\sigma}^{ij}$ and σ^{ij} are related by

$$\begin{aligned} \tilde{\sigma}^{11} &= \sigma^{11}\cos^2\varphi + \sigma^{22}\sin^2\varphi + \sigma^{12}\sin 2\varphi, \\ \tilde{\sigma}^{22} &= \sigma^{11}\sin^2\varphi + \sigma^{22}\cos^2\varphi - \sigma^{12}\sin 2\varphi, \\ \tilde{\sigma}^{12} &= (1/2)(\sigma^{22} - \sigma^{11})\sin 2\varphi + \sigma^{12}\cos 2\varphi. \end{aligned} \tag{2.1}$$

We express (1.4) in terms of the strain characteristics of the shell:

$$I_1 = 2[\tilde{e}_{11}\cos^2\varphi + \tilde{e}_{22}\sin^2\varphi], \quad I_3 = 2[\tilde{e}_{11}\sin^2\varphi + \tilde{e}_{22}\cos^2\varphi], \quad I_2 = (1/2)[(\tilde{e}_{11} - \tilde{e}_{22})\sin 2\varphi]^2. \tag{2.2}$$

Here we took into account that $\tilde{e}_{12} = 0$ because the shell's strain is axisymmetric. Using (1.3), (1.5), and (2.2), we express stresses (2.1) in the layer in terms of the strain characteristics of the shell $\tilde{e}_{11}$ and $\tilde{e}_{22}$, which are measured in an experiment. Then, we have

$$\begin{aligned} \tilde{\sigma}^{11} &= [A_{11}(I_1)I_1 + A_{13}(I_1)I_3](1 + \cos 2\varphi) \\ &+ [A_{31}(I_1)I_1 + A_{33}(I_3)I_3](1 - \cos 2\varphi) + A_2(I_2)(\tilde{e}_{11} - \tilde{e}_{22})\sin^2 2\varphi, \\ \tilde{\sigma}^{22} &= [A_{11}(I_1)I_1 + A_{13}(I_1)I_3](1 - \cos 2\varphi) \\ &+ [A_{31}(I_1)I_1 + A_{33}(I_3)I_3](1 + \cos 2\varphi) - A_2(I_2)(\tilde{e}_{11} - \tilde{e}_{22})\sin^2 2\varphi. \end{aligned} \tag{2.3}$$

Next, we use the equations of equilibrium

$$h\tilde{\sigma}^{11} = P/2\pi R, \quad h\tilde{\sigma}^{22} = qR, \tag{2.4}$$

where P is the external force acting along the axis of a cylindrical shell, q is the internal pressure in the shell, R is the radius of the middle surface of the shell, and h is the thickness of the shell.

The problem of determining the elastic characteristics $A_{11}(I_1)$, $A_{13}(I_1)$, $A_{31}(I_1)$, $A_{33}(I_3)$, and $A_2(I_2)$ from Eqs. (1.6), (2.3), and (2.4) is posed.

To this end, we expand the A_{ij} in series in certain systems of functions of the invariants I_k ($k = 1$, 2, 3):

$$A_{11}(I_1) = \sum_{k=0}^{N_1} A_{11}^k \psi_1^k(I_1), \quad A_{13}(I_1) = \sum_{k=0}^{N_2} A_{13}^k \psi_2^k(I_1), \quad A_{31}(I_1) = \sum_{k=0}^{N_3} A_{31}^k \psi_3^k(I_1),$$
$$A_{33}(I_3) = \sum_{k=0}^{N_4} A_{33}^k \psi_4^k(I_3), \quad A_2(I_2) = \sum_{k=0}^{N_5} A_2^k \psi_5^k(\hat{J}_2), \quad J_2 = \sqrt{I_2}. \tag{2.5}$$

In calculations, the powers of the invariants I_1, I_3, and J_2 were used as the functions ψ_i^j with $N_k = N = 2$ or $N = 3$. This corresponds to an approximation of the function A_{ij} by a quadratic or cubic parabola. Then, using relation (1.6), we express the A_{13}^k in terms of the A_{31}^k:

$$A_{13}^k = (1 + k)A_{31}^k, \quad k = 0, \ldots, N. \tag{2.6}$$

Equations (1.6), (2.3), and (2.4) can be written for each point of the loading trajectory $P(\zeta)$, $q(\zeta)$ (ζ is the loading parameter). Substituting relations (2.5) and (2.6) into (2.3), we obtain two linear algebraic equations for the A_{ij}^k for each value of the loading parameter.

The number of unknowns A_{ij}^k in the system of algebraic equations is defined by the order of approximation of the curves: $n = 4(N + 1)$.

The system of algebraic equations for the desired vector $X = \{A_{11}^0, A_{31}^0, A_{33}^0, A_2^0, \ldots\} = \{X^1, X^2, \ldots, X^n\}$ is written in matrix form as

$$Bx = C, \tag{2.7}$$

where $B = B(2m, n)$, $x = x(n)$, and $C = C(2m)$ (m is the number of measurements in the chosen experiments).

When $2m > n$, the system is overdetermined. To solve it, we use the mean-square residual minimization method:

$$\frac{\partial \delta^2}{\partial x} = 0, \quad \delta^2 = (Bx - C)^2.$$

This leads to an algebraic system of equations of order n, which is written in matrix form as

$$B_1 x = C_1. \tag{2.8}$$

Here $B_1 = B^t B$ and $C_1 = B^t C$ (B^t is a transposed matrix).

Theoretically, two experiments for different winding angles φ are sufficient to determine the linear elastic characteristics A_{11}^0, A_{33}^0, A_{13}^0, and A_2^0.

In this case, we readily obtain an expression for the 4×4 matrix of resolvent system (2.7) in the form

$$\det\|B_1\| = k(\beta_2 - \beta_1)(1 - \beta_1)(1 - \beta_2)[\tan^2 2\varphi_1 - \tan^2 2\varphi_2], \tag{2.9}$$

where k is a numerical coefficient, $\beta_1 = I_3^{(1)}/I_1^{(1)}$ corresponds to the first experiment, $\beta_2 = I_3^{(2)}/I_1^{(2)}$ corresponds to the second experiment, and φ_1 and φ_2 are the winding angles of a single tape for shells in the first and second experiments, respectively.

From expression (2.9) it follows that system (2.7) is solvable if the following conditions are satisfied: $\beta_1 \neq 1$, $\beta_2 \neq 1$, $\beta_1 \neq \beta_2$, and $\varphi_1 + \varphi_2 \neq \pi/2$. In the general case of a nonlinear-elastic composite material,

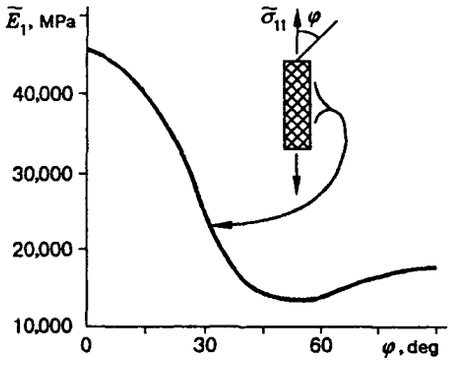

Fig. 2

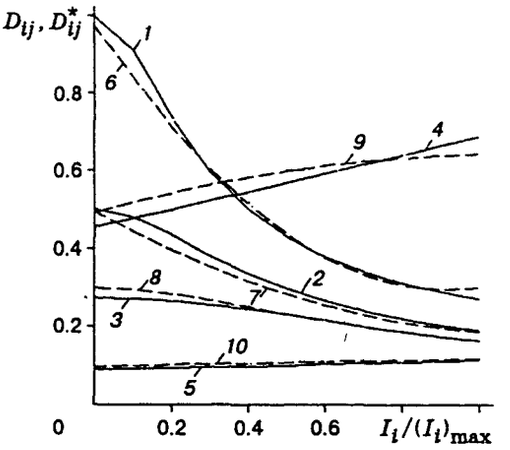

Fig. 3

derivation of degeneration conditions for matrix B_1 is a difficult problem.

Solution of system (2.7) for $N > 0$ involves difficulties due to the fact that the elements in this system differ from one another by many orders.

Therefore, in solution of system (2.7) we use normalization of columns by means of introduction of new unknowns $X^1_* = X^1\alpha_1, \ldots, X^5_* = X^5\alpha_5, \ldots$. There are various approaches to choice of α_n. Here we assume that $\alpha_n = \sum\limits_{i=1}^{m} |B_{in}|$. Then, we introduce a new matrix $B^*_{in} = B_{in}/\alpha_n$ in place of matrix B and normalize the rows in (2.7):

$$B^{**} = B^*_{in}/\gamma_i, \quad C^{**} = C_i/\gamma_i, \quad \gamma_i = \sum_{i=1}^{n} \left|B^*_{in}\right|.$$

After solving the system of equations $B^{**}X^* = F^{**}$, we determine the vector X:

$$X^i = X^*_i/\alpha_n.$$

When choosing shells for experiment, one should bear in mind that the winding angle plays a dominant role in determining the stiffness characteristics of shells [3, 4], as is seen from Fig. 2. Therefore, to determine more accurately the technical constants, one should choose shells in which winding angles differ greatly from one another.

3. The proposed method and the program developed were tested using the inverse-problem scheme. For a certain fictitious material, functions (1.5) were specified in explicit form and were used to calculate indications of force meters P and q and indications of strain gauges $\tilde{e}_{11}$ and $\tilde{e}_{22}$ from the known relations.

The thus-obtained experimental results were used as initial data to reconstruct functions (1.5) (in the form of their approximations). This method permitted us to investigate the influence of various factors (a spread in experimental data and an error in measuring the winding angle) on the accuracy of determining functions (1.5).

Test examples were studied for a nonlinear-elastic material characterized by the constitutive law

$$\begin{gathered} 4A_{11} = B_1(a/\sqrt{a^2 + e_{11}^2} + b), \quad 4A_{13} = \nu_{12}B_1(1 + 2e_{11}/a_1), \\ 4A_{33} = B_3(a/\sqrt{a^2 + e_{22}^2} + b), \quad 4A_{31} = \nu_{12}B_1(1 + e_{11}/a_1), \quad A_2 = 2B_2(a/\sqrt{a^2 + e_{12}^2} + b). \end{gathered} \tag{3.1}$$

Hence, when strains e_{11}, e_{22}, and e_{12} tend to zero, we have the following tangent stiffness characteristics:

$$\begin{gathered} 4A_{11}(0) = (1 + b)B_1, \quad 4A_{33}(0) = (1 + b)B_3, \quad A_2(0) = (1 + b)B_2, \\ 4A_{11}(0) = E_1/(1 - \nu_{12}\nu_{21}), \quad 4A_{33}(0) = E_2/(1 - \nu_{12}\nu_{21}), \quad G_{12} = A_2(0), \end{gathered} \tag{3.2}$$

TABLE 1

Experiment number	Winding angle $\pm\varphi$, deg	$e^{(k)}_{11,m}$	$e^{(k)}_{22,m}$
1	30	$0.0005m$	$0.0003m$
2	20	$0.0005m$	$0.0002m$
3	5	$0.0005m$	$0.0001m$

where E_1 and E_2 are the elastic moduli for longitudinal and transverse reinforcement, ν_{12} and ν_{21} are Poisson's ratios, and G_{12} is the shear modulus.

The parameters B_1, B_3, and B_2 appearing in (3.1) allow us to model both weak and strong material anisotropies. The following parameters were used for weak anisotropy:

$$B_1 = 10^5\,\text{MPa},\quad B_3 = 5\cdot 10^4\,\text{MPa},\quad \nu_{12} = 0.1,\quad B_2 = 3\cdot 10^4\,\text{MPa},\quad a = 10^{-3},\quad a_1 = 2\cdot 10^{-2},\quad b = 0.1. \tag{3.3}$$

Then, strain values in a single tape with winding angle $\varphi(k)$ were specified. The loading number m was taken as the loading parameter ζ:

$$e^{(k)}_{11,m} = e^{(k)}_{10}m,\quad e^{(k)}_{22,m} = e^{(k)}_{20}m,\quad m = 1, 2, \ldots, m_1.$$

Here $e^{(k)}_{10}$ and $e^{(k)}_{20} \ll 1$ were taken arbitrarily. The value of $e^{(k)}_{12,m}$ was calculated from the symmetry condition for the strain deformation of the shell

$$\tilde{e}^{(k)}_{12,m} = (1/2)(e^{(k)}_{22,m} - e^{(k)}_{11,m})\sin 2\varphi + e^{(k)}_{12,m}\cos 2\varphi = 0.$$

Expressions similar to (2.1) were used to determine $\tilde{e}_{11}$ and $\tilde{e}_{22}$ and also indications of strain gauges. Stresses in the tape were calculated by expressions (1.3), (1.5), and (3.1), and stresses in the shell with the given winding angle were calculated by relations (2.1). Finally, the external loads $P^{(k)}$ and $q^{(k)}$ for given values of $h^{(k)}$ and $R^{(k)}$ were determined by relations (2.4). The experimental results for $m = 10$ are listed in Table 1.

To obtain these functions using the proposed method, we used their representations in the form

$$\begin{gathered} A_{11} \approx A^*_{11} = A^0_{11} + A^1_{11}I_1 + A^2_{11}I_1^2,\quad A_{33} \approx A^*_{33} = A^0_{33} + A^1_{33}I_3 + A^2_{33}I_3^2, \\ A_{13} \approx A^*_{13} = A^0_{13} + A^1_{13}I_1 + A^2_{13}I_1^2,\quad A_2 \approx A^*_2 = A^0_2 + A^1_2J_2 + A^2_2J_2^2 \end{gathered} \tag{3.4}$$

(A^k_{ij} and A^k_j are unknown constants).

Figure 3 ($k_{11} = 1$, $k_{33} = 1$, $k_2 = 0.25$, $k_{13} = 5$, and $k_{31} = 1$) shows graphs of the functions (3.4) and the corresponding graphs of the initial functions (3.1). In Fig. 3 and the other figures, $D_{ij} = k_{ij}A_{ij}/A^0_{11}$, $D^*_{ij} = k_{ij}A^*_{ij}/A^0_{11}$ (k_{ij} are scaling factors which are chosen so as to show parameters differing in magnitude in one graph), curves 1–5 correspond to the functions D_{11}, D_{33}, D_2, D_{13}, and D_{31}, and curves 6–10 to the functions D^*_{11}, D^*_{33}, D^*_2, D^*_{13}, and D^*_{31}.

As $e_{ij} \Rightarrow 0$, we have $4A^0_{11} = 1.0736\cdot 10^5$ MPa, $4A^0_{13} = 1.08\cdot 10^4$ MPa, $4A^0_{33} = 5.4246\cdot 10^4$ MPa, and $A^0_2 = 3.014\cdot 10^4$ MPa. These values coincide with sufficient accuracy with those specified in (3.1) and (3.3). The results obtained show that for the tested material (3.1) with weak anisotropy (3.3) and idealized experiments, formulas (3.4) can be used with sufficient accuracy over the entire range of deformation.

For strong anisotropy, the following values were assumed in relations (3.1):

$$\begin{gathered} B_1 = 10^5\,\text{MPa},\quad B_3 = 10^4\,\text{MPa},\quad \nu_{12} = 0.01,\quad B_2 = 3\cdot 10^3\,\text{MPa}, \\ a = 10^{-3},\quad a_1 = 2\cdot 10^{-2},\quad b = 0.1. \end{gathered} \tag{3.5}$$

The experimental data given in Table 2 were used for $m = 1, \ldots, 10$. The values of A^*_{ij} obtained from (3.4) are presented in Fig. 4 ($k_{11} = 1$, $k_{33} = 10$, $k_2 = 1$, $k_{13} = 20$, and $k_{31} = 40$).

4. Use of approximation function (3.4) over the entire deformation range leads, as a rule, to discrepancy between A^0_{ij} and the corresponding linear-elastic constants for small strains. This is due to the fact that the stress–strain curve is approximated using the condition of minimum mean-square residual over the entire range

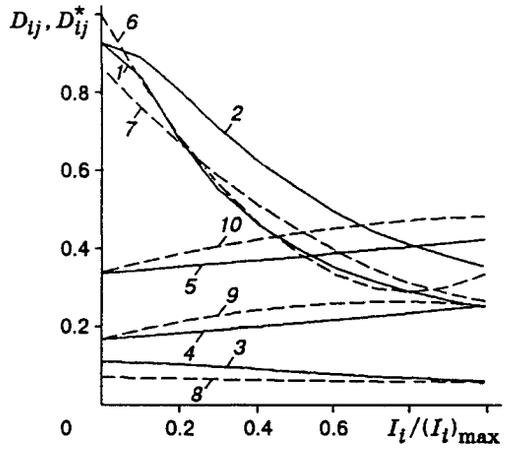

Fig. 4

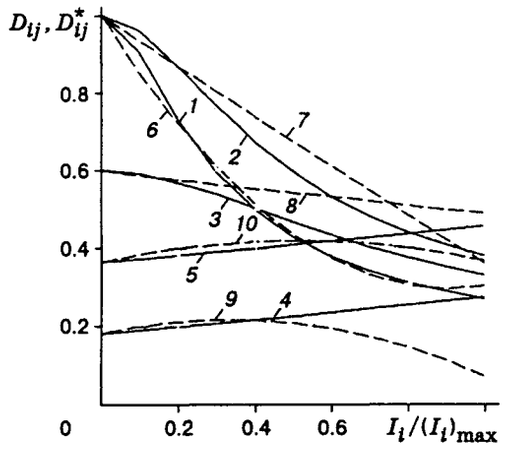

Fig. 5

of variation of the arguments. If it is necessary that the linear elastic characteristics coincide with values of A^0_{ij} for zero arguments, the following approach can be proposed. First, the linear-elastic characteristics $A_{ij(e)}$ are determined for $e^{(k)}_{ii,m} \Rightarrow 0$. Then, system (2.7) subject to the condition $A^0_{ij} = A_{ij(e)}$ is transformed.

Figure 5 ($k_{11} = 1$, $k_{33} = 10$, $k_2 = 5$, $k_{13} = 20$, and $k_{31} = 40$) shows the calculation results that begin to deviate considerably from exact results as e_{ij} increase.

An analysis of these and the other results obtained (Figs. 3–5) shows that use of power series (3.4) for the entire range of argument variation is justified for weak anisotropy and smoothly varying functions A_{ij}. However, the approximation by higher-order polynomials leads to an ill-conditioned matrix B_1 and oscillations of approximation functions. Therefore, for materials with strong anisotropy, one should either change the method, of determining stiffness characteristics or use other systems of functions (for example, spline functions). In the first method, it is possible to improve the method of determining A_{ij} by a double approximation of the unknown functions. The essence of this method is as follows. We divide the interval of variation of ζ into subintervals $\Delta\zeta^{(k)}$ in which the unknown functions are approximated by low-order polynomials. Writing the equations of equilibrium (2.7) only for the points lying in this interval, we can find the functions A^*_{ij}. In the entire interval of variation of ζ we obtain a piecewise-continuous function. Having the values of these functions in the middle of the intervals $\Delta\zeta^{(k)}$, we can perform a second approximation of these functions by, for example, spline functions and obtain continuous functions A^{**}_{ij}. It is expedient here to use approximation methods that not only minimize the deviation of A^{**}_{ij} from A^*_{ij} but also limit the curvature of A^{**}_{ij}.

The proposed double approximation method was realized in an automatic experimental-data processing system. Figure 6 ($k_{11} = 1$, $k_{33} = 10$, $k_2 = 1$, $k_{13} = 20$, and $k_{31} = 40$) shows the calculation results for material (3.1) with strong anisotropy (3.5) from experiment Nos. 2, 4, and 7 (see Table 2) for three equal subintervals. The results exhibit good agreement between the approximations obtained and functions (3.1).

5. To analyze the effect of spread of experimental data on stiffness characteristics, the above test problems were used. A spread in input parameters was introduced in the initial data. The effect of these perturbations on the coefficients $A^{(k)}_{ij}$ was studied. An analysis of the numerical experiments leads to the following conclusions:

(1) the higher the degree of anisotropy (E_1/E_2), the stronger the effect of the spread in the geometrical and loading parameters $\delta\varphi$, δR, δh, δP, and δq on $A^{(k)}_{33}$, $A^{(k)}_2$, and $A^{(k)}_{31}$;

(2) the function A_{11} is the most stable against the perturbations, while the functions A_{13} and A_{31} are the least stable.

We now analyze in more detail the effect of spread of experimental data on the stiffness characteristics

TABLE 2

Experiment number	Winding angle $\pm\varphi$, deg	$e^{(k)}_{11,m}$	$e^{(k)}_{22,m}$
1	44	$0.0005m$	$0.00035m$
2	30	$0.0005m$	$0.00030m$
3	25	$0.0005m$	$0.00025m$
4	20	$0.0005m$	$0.00020m$
5	15	$0.0005m$	$0.00015m$
6	10	$0.0005m$	$0.00010m$
7	5	$0.0005m$	$0.00005m$

TABLE 3

Experiment number	Winding angle $\pm\varphi$, deg	$e^{(k)}_{11,m}$	$e^{(k)}_{22,m}$
1	35	$-0.0002m$	$0.0004m$
2	55	$-0.0003m$	$0.0002m$
3	65	$-0.0003m$	$0.0004m$
4	70	$-0.0002m$	$0.0005m$
5	25	$-0.0001m$	$0.0003m$

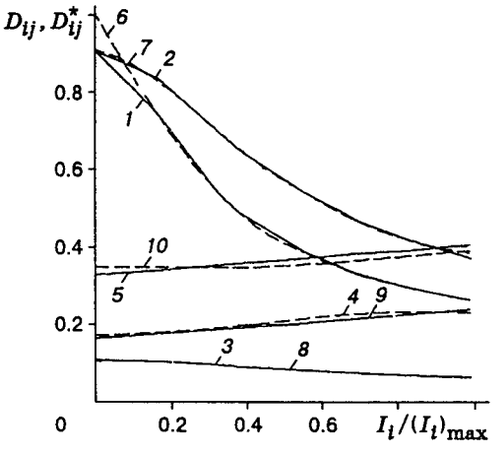

Fig. 6

of a composite material for the problem of determining linear-elastic constants for the constitutive law

$$\sigma^{11} = 4A_{11}(0)e_{11} + 4A_{13}(0)e_{22}, \quad \sigma^{22} = 4A_{13}(0)e_{11} + 4A_{33}(0)e_{22}, \quad \sigma^{12} = 2G_{12}e_{12} \tag{5.1}$$

where $4A_{11}(0) = 10^4$ MPa, $4A_{33}(0) = 5 \cdot 10^2$ MPa, $4A_{13}(0) = 10^2$ MPa, and $G_{12} = 300$ MPa.

Table 3 lists the calculated experimental values of strains and external forces for $m = 1, \ldots, 10$.

Calculations show that, as in [4], a small spread in the initial data (a few percent) can lead to large variations in values of Poisson's ratio ν_{12} and even to a change of sign.

Table 4 gives the changes in the stiffnesses of CM versus the measurement error for the winding angle in one of the experiments. Exact values of the stiffness characteristics are listed in the first row. The second, third, and fourth rows give, respectively, the results for experiment No. 1, in which an angle of 26° was used in place of an angle of 25°, the results for experiment No. 5, in which an angle of 73° was used, and the results for the case of errors ($\Delta\varphi_1 = -1°$) and ($\Delta\varphi_5 = 3°$) in experiment Nos. 1 and 5. It is seen from Table 4 that the quantities A^0_{11} and A^0_2 vary only slightly, while the variation of A^0_{33} is more pronounced, and the variation of A^0_{13} is considerable.

We now consider the effect of measurement errors for $\tilde{e}_{11}$, $\tilde{e}_{22}$, $\tilde{\sigma}^{11}$, and $\tilde{\sigma}^{22}$ by varying E_1 or E_2 by 10 or 20% in preparing initial data in one experiment. The calculation results are shown in Table 5. Row 1 gives the elastic characteristics for the case where a 20% error for E_2 was introduced in preparing initial data for experiment No. 1 ($\varphi = 25°$), and row 2 gives that for experiment No. 5 ($\varphi = 70°$). The results presented in rows 3 and 4 correspond to the case where a 10% error for E_1 was introduced in preparing initial data for experiment Nos. 1 ($\varphi = 25°$) and 5 ($\varphi = 70°$), respectively.

An analysis of Table 5 shows that the effect of perturbations in experimental data for $\tilde{e}_{11}$, $\tilde{e}_{22}$, $\tilde{\sigma}^{11}$, and $\tilde{\sigma}^{22}$ on A^0_{ij} is similar to the effect of perturbations for angle φ.

TABLE 4

$4A_{11}^0$	$4A_{13}^0$	$4A_{33}^0$	A_2^0	Measurement error of winding angle φ_1
GPa				
10,000	100	500	300	
9964	−20	470.4	296	$\Delta\varphi_1 = 1°$
9956	298.6	511.6	315.5	$\Delta\varphi_5 = 3°$
10,000	414	547.2	319.2	$\Delta\varphi_1 = -1°$, $\Delta\varphi_5 = 3°$

TABLE 5

$4A_{11}^0$	$4A_{13}^0$	$4A_{33}^0$	A_2^0
GPa			
10056	133.16	546.4	300.2
10052	97.04	557.2	293.1
9936	−35.2	446	295.2
9976	−23.3	449.6	295.9

TABLE 6

Winding angle $\pm\varphi$, deg	E_2, GPa	
	calculation	experiment
35	6.96	7.8
55	20.8	15.8
65	43.9	40
70	58.7	50

The significant effect of measurement errors on the values of A_{13}^0, A_{33}^0, and A_2^0 is caused by the fact that the desired vector $X = \{A_{11}^0, A_{13}^0, A_{33}^0, A_2^0\}^t$ contains components that can differ from one another by several orders. In our case, A_{11}^0 is the maximum element. Therefore, an insignificant variation of A_{11}^0 in the equations of equilibrium can be compensated only by considerable variations of A_{13}^0, A_{33}^0, and A_2^0. Let the initial data differ from statistically exact values by the quantity $\delta = \Delta b$, where b is the vector of the initial exact data. If the system of equations is well conditioned with respect to the vector X, the deviation of the vector X from the exact value will be on the same order: $\|\Delta X\| = k\|\delta\|$ and $k \sim 1$. However, since the difference between the values of components of the vector X is large (about two orders for UCM), the variation of small components will be very significant. Suppose, for example, that $X_2 \sim X_1 \cdot 100$ and $\|\Delta X\| \sim 0.05$ (5%). Assuming that $\|\Delta X_2\| \sim \|\Delta X\|$, we have $\|\Delta X_2\| \sim \|X_2\|$. Thus, even small deviations of initial data from exact values can lead to considerable variations of X_2.

6. The method described above was employed in processing concrete experiments performed on a setup which was designed and manufactured at the Kazan' State Architect-Building Academy to investigate the mechanical properties of fibrous composites on tubular specimens (cylindrical shells) [6, 7]. The setup was supplied with an automated strain-measurement and experimental-data-processing system. The operation of the system involves three stages. In the first stage, longitudinal and circumferential stresses and strains in tubular specimens are calculated using indications of strain and force gauges. In the second stage, the results for specimens of one family (the same winding angles and the same loading paths) are averaged, and the required dependences for each series of tested specimens are approximated and smoothed by means of spline functions. In the third stage, the loading parameter is chosen and functions (2.8) approximating the stiffness characteristics A_{ij} are determined.

The experimental-data-processing system with a complete set of service programs, including graphic programs, is realized on a PC. Experimental data for internal pressure, winding angles of $\pm\varphi = 35$, 55, 65, and 70°, and thicknesses of 1.5–2 mm were used. Evidently, over a wide range of deformation, the graphs plotted by the deformation results are linear in the component $\tilde{e}_{22}$, which was used as the loading parameter. Therefore, the linear-elastic characteristics $4A_{11}^0 = 98.84$ GPa, $4A_{13}^0 = A_{31}^0 = 1.35$ GPa, $4A_{33}^0 = 3.100$ GPa, and $A_2^0 = 3.10$ GPa, and also the technical constants $\nu_{12} = A_{13}^0/A_{11}^0 = 0.0137$, $\nu_{21} = A_{13}^0/A_{33}^0 = 0.435$, $E_1 = 4A_{11}^0(1 - \nu_{12}\nu_{21}) = 98.25$ GPa, $E_2 = 4A_{20}^0(1 - \nu_{12}\nu_{21}) = 3.08$ GPa, and $G = A_2^0 = 3.10$ GPa were

determined.

To estimate the results indirectly, the stiffness characteristics of the shells $\tilde{E}_2 = \tilde{\sigma}^{22}/\tilde{e}_{22}$ were found from the experimental data and also by calculating A^0_{ij} from the relations [8]

$$\tilde{E}_2 = 4\tilde{A}_{33}(1 - \tilde{\nu}_{12}\tilde{\nu}_{21}),$$

$$4\tilde{A}_{11} = 4A^0_{11}\cos^4\varphi + 4A^0_{33}\sin^4\varphi + 2(4A^0_{13} + 2A^0_2)\sin^2\varphi \cdot \cos^2\varphi,$$

$$4\tilde{A}_{33} = 4A^0_{11}\sin^4\varphi + 4A^0_{33}\cos^4\varphi + 2(4A^0_{13} + 2A^0_2)\sin^2\varphi \cdot \cos^2\varphi,$$

$$4\tilde{A}_{13} = 4A^0_{13} + [4A^0_{11} + 4A^0_{33} - 2(4A^0_{13} + 2A^0_2)]\sin^2\varphi \cdot \cos^2\varphi,$$

$$\tilde{\nu}_{12} = \tilde{A}_{13}/\tilde{A}_{11}, \quad \tilde{\nu}_{21} = \tilde{A}_{13}/\tilde{A}_{33}.$$

The results of comparison are given in Table 6.

Thus, the proposed method makes it possible to determine the stiffness characteristics of UCM by processing data of tests on thin-walled structural members made of this UCM. The difference between the calculation results (obtained by the above method) and experimental results does not exceed 25%.

This work was supported by the Russian Foundation for Fundamental Research (Grant 93-01-16747).

REFERENCES

1. I. G. Teregulov, "Finite strains of thin anisotropic and composite shells and constitutive relations," *Mekh. Kompozit. Mater.*, No. 4, 654–660 (1987).
2. I. G. Teregulov, "Constitutive relations for anisotropic and fibrous composite shells for finite strains," *Izv. Akad. Nauk SSSR, Mekh. Tverd. Tela*, No. 3, 167–173 (1989).
3. N. A. Alfutov, P. A. Zinov'ev, and B. G. Popov, *Calculation of Multilayer Composite Plates and Shells* [in Russian], Mashinostroenie, Moscow (1984).
4. N. A. Alfutov, P. A. Zinov'ev, and L. P. Tairova, "Identification of the elastic charateristics of unidirectional materials using results of tests of multilayer composites," in: *Strength Calculations* [in Russian], No. 30, Mashinostroenie, Moscow (1989).
5. L. Barther, H. Berger, J. P. Chaquin, and R. Ohayon, "Identification des caracteristiques mecaniques des structures en materian composite," *Rech. Aerosp.*, No. 5, 327–332 (1981).
6. I. G. Teregulov, K. P. Alekseev, A. L. Til'sh, and V. M. Chernov, "Experimental determination of mechanical properties of organic-plastics using thin-walled tubular specimens under axial tension and compression, Ser. VIII," *Materialoved. Mekh. Kompozit. Mater.*, No. 2, 4–12 (1993).
7. I. G. Teregulov, K. P. Alekseev, D. Kh. Safiullin, and R. A. Kayumov, "A setup for investigating the mechanical properties of fibrous composites on tubular specimens," *Mekh. Kompozit. Mater.*, **31**, No. 1, 125–130 (1995).
8. V. V. Vasil'ev, *Mechanics of Structures of a Composite Material* [in Russian], Mashinostroenie, Moscow (1988).